HYDRATION PROCESS OF FLY ASH BLENDED CEMENT COMPOSITE

K. MOHANRAJ[*], G. SIVAKUMAR[a] and S. BARATHAN[b]

Department of Physics, Manonmanian Sundaranar University, TIRUNELVELI - 627012 (T.N.) INDIA
[a]Centralised Instrumentation and Service Laboratory (CISL), Annamalai University,
ANNAMALAINAGAR (T.N.) INDIA
[b]Department of Physics, Annamalai University, ANNAMALAINAGAR- 608 002 (T.N.) INDIA

ABSTRACT

In the present investigation, to evaluate the performance of a 25% cement replacement by fly ash (FA), blended composite and control (without FA) was hydrated with sea water (SW) with the water to binder ratio 0.4. Intervals of the hydrated samples are 1 hour, 6 hours, 7 hours, 1 day, 7 days, 28 days, 90 days and 180 days. Setting time and compressive strength of control and blended composites were carried out. The hydrated samples were subjected to FTIR and SEM with EDS analysis.

This study reveals that the control (without fly ash) pastes can accelerate the early stage of hydration due to higher amounts of ettringite formation and retarded hydration process in later periods due to $Ca(OH)_2$ product reacting with sodium, magnesium and chloride ions to form recrystallised gypsum and $Mg(OH)_2$. These products are deteriorating in control paste. In blended composite, these products are free due to pozzolanic reaction of fly ash consuming $Ca(OH)_2$. Also, the Al_2O_3 rich in fly ash reacts with chloride to form Friedel's salt ($C_3A.CaCl_2.10H_2O$). This reduces the amount of free chlorides and hence, the blended composite has higher strength than control in later periods and increase the resistance to sulphate attack.

Key words: Fly ash, Cement, Sea water, FTIR, SEM

INTRODUCTION

Fly ash is a by-product of coal in thermal power stations. By combining ordinary portland cement (OPC) with fly ash (FA), blended cement can be formed. The pozzolanic reactivity of fly ash is well recognized and has led it to use as supplementary cementing material in concrete. Usage of fly ash has three main advantages such as (i) the use of a zero cost raw material, (ii) the conservation of natural resources and (iii) the elimination of waste[1].

_____

[*]Author for correspondence; Ph.: (M) : 91-9788083079; E-mail: km_aup@yahoo.co.in

Coal-based thermal power installations in India contribute about 65% of the total installed capacity for electricity generation and producing ash content of about 35-45%. Presently, about 110 million tones of coal-ash is generated from more than 70 thermal power plants[2]. The variation in the properties of fly ash and fly ash blended cement through different concentrations of fly ash under Indian condition is meagre. Also the utility of the sea water in the blend is of considerable interest. FTIR better characterizes the amorphous and poorly crystalline phases that occur in blended cement. SEM with EDS has been widely used to study and visually see the formation of hydration products and its composition. Thus, the present study is aimed at in evaluating the performance of fly ash blended cement paste using seawater (SW) and to understand the relationship between compressive strength and molecular vibration changes and microstructural changes using FTIR and SEM.

EXPERIMENTAL

Materials and methods

ASTM type I market available ordinary portland cement (OPC) and fly ash (FA) collected from Mettur Thermal power station, Tamil Nadu, India were used in this study and its chemical analysis is given in Table 1.

Table 1: Chemical analysis of the OPC and fly ash

Compd.	CaO	SiO$_2$	Al$_2$O$_3$	Fe$_2$O$_3$	SO$_3$	MgO	Na$_2$O	K$_2$O	LOI	others
OPC	63.0	21.9	5.75	3.25	2.35	1.97	0.50	0.28	1.0	-
Fly ash	2.82	60.78	24.10	6.0	0.14	1.07	0.84	0.87	1.78	1.60

According to the ASTM C-618, it is a Class 'F' fly ash and 25% of ordinary portland cement is replaced by it as this percentage is suggested by many workers[3,4]. The control (0% FA) and blended composites (OPC+25%FA) were hydrated with seawater collected from Bay of Bengal at Pichavaram, Tamil Nadu, India. Concentration (in ppm) of major ions are Na (9000), K (260), Ca (2400), Mg (312), Cl (14,168) and SO$_4$ (1810). Water to binder ratio of (w/b) 0.4 at different intervals like 1 hour, 6 hours, 7 hours, 1 day, 7 days, 28 days, 90 days and 180 days.

The pelletised sample with KBr was used for recording FTIR spectra (4000-400 cm^{-1}) using Perkin-Elmer-RX1 FTIR spectrometer. A thin layer of fractured surface of hydrated sample was mounted on the specimen stub using double side adhesive carbon tape for

monitoring surface morphology. The samples were coated with the help of gold coater (JEOL auto fine coater model JFS-1600; coating time is 120 sec. with 20mA). Scanning electron micrographs were recorded using JEOL-SEM Model JSM – 5610 LV with an accelerating voltage of 20 KV at high vacuum mode and secondary electron image. FTIR can provide direct information on the structural and compositional characteristics of the blend in a relatively simple way. SEM has been widely used to study and visually see the formation of hydration products (CSH_2, CSH, CH and etc.) of the paste. Setting time and compressive strength of the samples were carried out using ASTM C 191 and 109 procedure and its results are given in Fig. 1(a) and (b)[5,6].
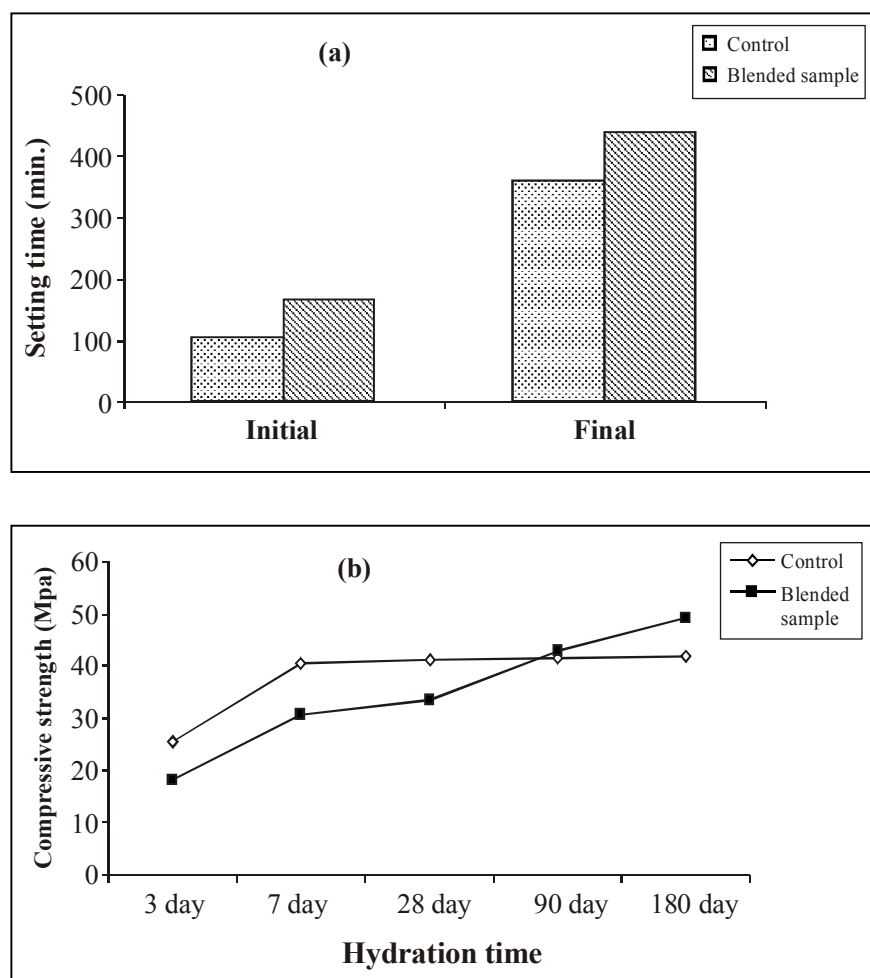

Fig. 1: (a) Setting and (b) Compressive strength of the control and blended composites

RESULTS AND DISCUSSION

FTIR study

FTIR spectra of control and blended composites hydrated with sea water are shown in the Figs. 2 and 3, respectively. In 1 hour control (Fig. 2a) spectrum, a medium and broad band centred at 3401 cm^{-1} is due to symmetric stretching vibration (v_1 H_2O) of adsorbed water molecules and weak band observed around 1630 cm^{-1} may be due to in-plane-bending (v_2 H_2O) vibration of water molecules[7]. A band having strong intensity at 1425 cm^{-1} is assigned to asymmetric stretching vibration (v_4) and a weak band at 874 cm^{-1} is due out-of-plane bending (v_4) vibration of carbonate bands due to absorbance of CO_2 from atmosphere[8]. A strong triplet band between 1142 and 1115 cm^{-1} can be assigned to v_3 vibration of sulphate ($v_3\,SO_4^{2-}$). Also, a weak doublet observed in lower region (around 658 and 617 cm^{-1}) is due to out-of-plane ($v_4\,SO_4^{2-}$) and in-plane bending ($v_2\,SO_4^{2-}$) vibrations of sulphate, respectively[9].
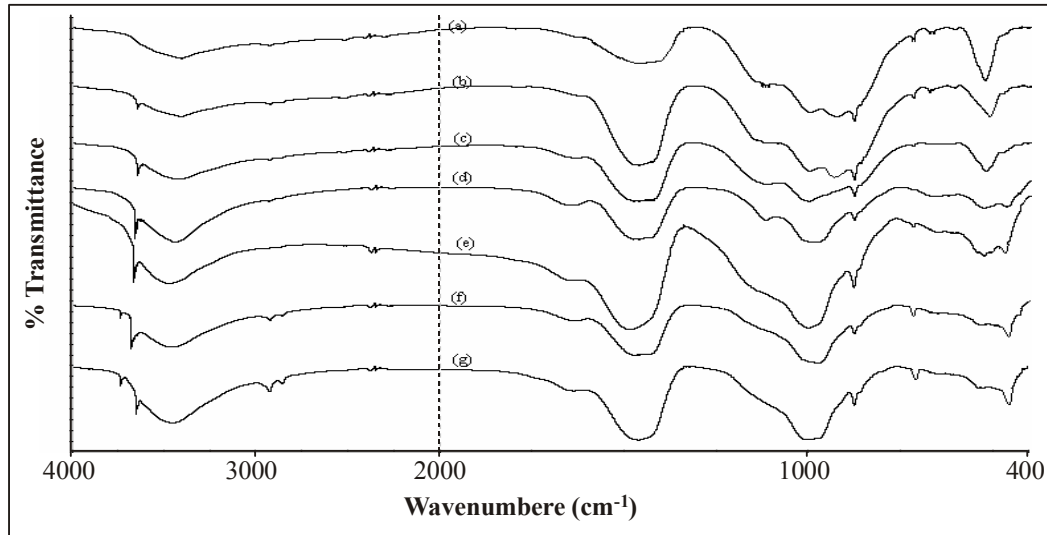

Fig. 2: FTIR spectra of control sample for (a) 1 hour, (b) 6 hours, (c) 1 day, (d) 7 days, (e) 28 days, (f) 90 days and (g) 180 days

Dynamics of changes in the sulphate bands is important one. Changes in intensity of the bands can provide valuable information on mechanism occurring in early hydration. The faster decreasing rate of triplet sulphate band is an indication of ettringite formation[10]. This product indicates that the control paste start setting. Ettringite formation is the reaction of

C$_3$A and gypsum with water and the essential equation is,

$$C_3A + 3\ C\bar{S}H_2 + 26H \rightarrow C_6A\bar{S}_3H_{32}\ \text{(Ettringite)} \qquad ...(1)$$

A broad and strong band around 920 cm^{-1} is due to asymmetric stretching vibration (ν_3 SiO$_4^{4-}$) of C$_3$S and a medium intensity peak observed at 846 cm^{-1} is due to C$_2$S. In lower region, a strong and sharp peak observed at 520 cm^{-1} is due to out-of-plane-bending (ν_4 SiO$_4^{4-}$) vibration of C$_2$S and a weak peak observed at 469 cm^{-1} is due to in-plane-bending (ν_2 SiO$_4^{4-}$) vibration of C$_3$S[10].

A weak shoulder is observed at 700 cm^{-1} may be related to the presence of C$_3$A, while no specific assignments could be made to the C$_4$AF phase in the OPC[11]. At final setting time (6th hour) spectrum (Fig. 3b), a shoulder is emerging at 3640 cm^{-1}, which may be due to the formation of Ca(OH)$_2$[12]. The ν_3 sulphate (triplet) merges to form a singlet at 1125 cm^{-1} and the ν_4 and ν_2 doublets form a singlet. Also, the ν_1 and ν_2 water bands having a stronger intensity with a shift to higher wave number around 3438 cm^{-1} and 1635 cm^{-1} are observed. These changes indicate the conversion of ettringite to monosulphate[13]. This shows the conversion from plastic to hardened state and coincides with the setting observation (Fig.1a) and its essential reaction (Eq. 2) is
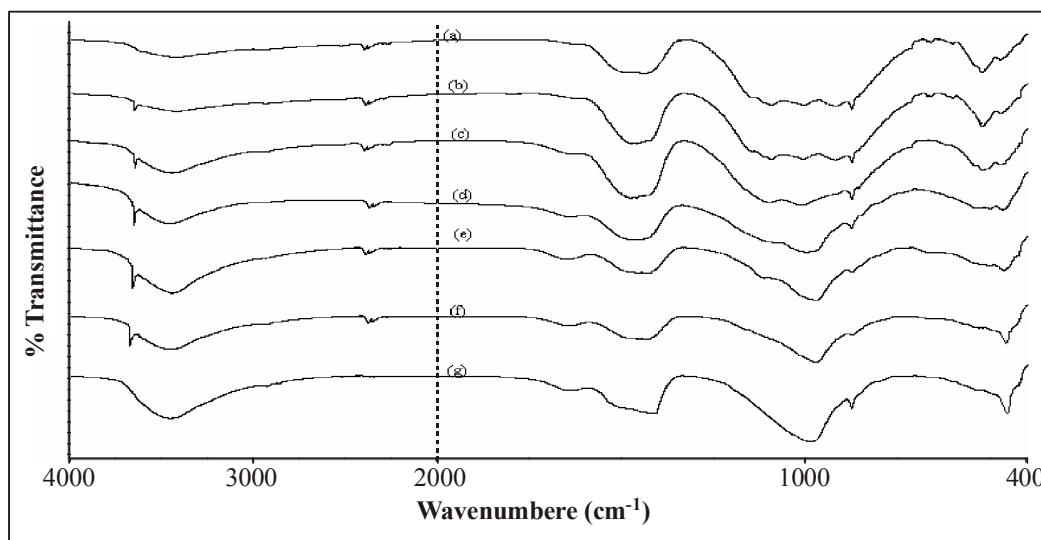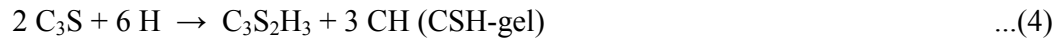
$$2\ C_3A + C_6A\bar{S}_3H_{32} + 4\ H \rightarrow 3\ C_4ASH_{12} \qquad ...(2)$$

Fig. 3: FTIR spectra of blended composite for (a) 1 hour, (b) 7 hours, (c) 1 day, (d) 7 days, (e) 28 days, (f) 90 days and (g) 180 days

Hydration reactions of C_4AF is similar to C_3A, but aluminium in the reaction products may be replaced by iron and also an iron/aluminium-hydroxide is formed (Eq. 3).

$$C_4AF + 9\ H\ \rightarrow\ C_4(A,F)H_6 + (A,F)H_3 \qquad\qquad ...(3)$$

At 1 day spectrum (Fig. 3c), the ν_3 silicate band at 920 cm^{-1} shifts to higher wavenumber at 985 cm^{-1}. It is due to formation of calcium silicate hydrate (CSH)[14], which is responsible for the strength of the paste (Eq. 4 and 5).
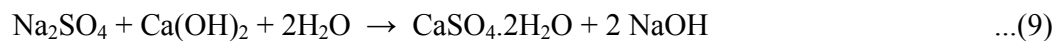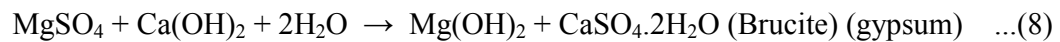
$$2\ C_3S + 6\ H\ \rightarrow\ C_3S_2H_3 + 3\ CH\ (CSH\text{-gel}) \qquad\qquad ...(4)$$

$$2\ C_2S + 4\ H \rightarrow C_3S_2H_3 + CH \qquad\qquad ...(5)$$

Cement chemistry notation: $C = CaO$; $S = SiO_2$; $A = Al_2O_3$; $F = Fe_2O_3$; $S = \overline{S}O_3$ and $H = H_2O$

The sulphate and aluminate bands have markedly reduced in intensity in 1 day. The ν_1 and ν_2 water bands (3438 cm^{-1} and 1635 cm^{-1}) and $Ca(OH)_2$ peak gets increasing intensity with time. Also, the carbonate bands slightly increase in intensity with time elapse as CO_2 reacts with CH and CSH producing calcium carbonate as follows (Eq. 6 and 7).

$$CH + CO_2\ \rightarrow\ CaCO_3 + H_2O \qquad\qquad ...(6)$$

$$CSH + CO_2\ \rightarrow\ CaCO_3 + SiO_2 + H_2O \qquad\qquad ...(7)$$
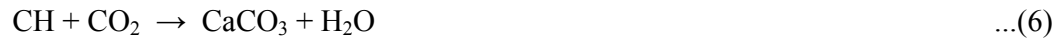
This result is supported by the observation of Van Grevan et al.[15], who suggested that the carbonation reactions are rapid but later these become slow as time increases. At 28th day, the relative intensity change of the silicate bands (ν_4 decreases while ν_2 increases) is slow. After 28 days, the silicate bands have lesser intensity. The CH peak is also slightly less in intensity as control paste reacts with sodium, magnesium ions etc. in seawater. A new peak around 3696 cm^{-1} and the sulphate band (658 cm^{-1}) is observed in 90th and 180th day spectra. It may be due to $Mg(OH)_2$[16] and recrystallisation of gypsum peak[17]. $Mg(OH)_2$ (brucite) is produced by the reaction with Mg^{2+} ions and CH. The role of Na_2SO_4 in seawater may produce the main hydration product, recrystallisation of gypsum and ettringite. Depending on lime availability, CH interacts with Na_2SO_4 to form these secondary products through the reaction (Eq. 8 and 9).

$$MgSO_4 + Ca(OH)_2 + 2H_2O\ \rightarrow\ Mg(OH)_2 + CaSO_4.2H_2O\ (\text{Brucite})\ (\text{gypsum}) \quad ...(8)$$

$$Na_2SO_4 + Ca(OH)_2 + 2H_2O\ \rightarrow\ CaSO_4.2H_2O + 2\ NaOH \qquad\qquad ...(9)$$

The role of $MgSO_4$ in sea water, may cause the deterioration of the hydration products due to formation of gypsum and brucite ($Mg(OH)_2$. The above said reactions, CH is well known to be responsible for the formation of gypsum, and gypsum is known to be the first step of the formation of secondary ettringite, which can be considered as the principal cause of deterioration[18]. Also, the free chloride dissolved in the pore water (alkanity) causes the corrosion of paste's structure. These products may cause the deterioration of the hydration products. Thus, the control has a less intensity of CSH at later stages (180 days) and coincides with compressive strength observation (Fig. 1b).

Blended composite

Comparing the Fig. 3, the hydration reaction of blended composite seems to be similar as that of control (Fig. 2) with a variation in reaction rate. A broad and strong band observed at 1096 cm^{-1} and a small peak at 795 cm^{-1} are due to T-O stretching vibration of characteristic fly ash band (T = Si and Al)[19]. The sulphate and water band changes (i.e. ettringite to monosulpahte conversion) are observed at 7th hour spectrum (1 hour later than control) due to the consumption of sulphate and C_3A compared to control. According to Gjørv and Vannsland[20]. Portland cement offers chloride penetration higher than blended cement. Also, the formation of ettringite acting as a coating layer around grains is more crystallised. Hence, the reaction is faster in control paste than blended cement paste. The acceleration hydration of control is due to the predominance of chloride ions tending to accelerate the hydration process of OH^- and Ca^{2+} ions[21]. The delay of setting of the blended composite is coinciding well with the Vicat's observation (Fig. 1b). The shift of water bands are also less compared to control.

In 1 day (Fig. 4c) spectrum, the v_3 silicate band is shifted to higher wavenumber at 980 cm^{-1} with less intensity than control due to less amount of CSH. At 28th day (Fig.3e), the $\square_\square$ silicate band gets increasing intensity while the CH peak (3640 cm^{-1}) and characteristic fly ash band (1096 cm^{-1}) gets a decreasing in intensity. It may be due to starting of pozzolanic reaction of fly ash and produce secondary CSH into the paste (Eq. 8)

$$3\ Ca(OH)_2 + 2\ SiO_2 + H_2O\ \rightarrow\ 3CaO.2SiO_2.3H_2O\ \text{(Secondary CSH)} \qquad ...(10)$$

In blended paste, the pozzolanic activity of fly ash consumes the quantity of CH due to the pozzolanic reaction (Eq. 10); so, CH is no longer available for reaction with sulphates. This prevents the formation of secondary products (gypsum, ettringite and brucite). A rapid change in carbonation (decrease in intensity) occurs after 28 days and slows down. This may be attributed to the $CaCO_3$ reacting with $Ca(OH)_2$ and fly ash. This forms a complex of $CaSiO_3.CaCO_3.Ca(OH)_2.nH_2O$ and promote the formation of CSH[22]. According to Shi et

al.[23], the Na_2SO_4 accelerated the reaction of fly ash through the reaction (Eq. 9). The generated NaOH increased the pH of the solution and speed up the pozzolanic reaction between $Ca(OH)_2$ and fly ash. This may be one of the reason for blended composite to have an increasing strength after 28 days.

As time passes (at 180th day), the v_3 silicate band (990 cm^{-1}) has a stronger intensity with a higher shift (5 wavenumbers higher than control) and the relative intensity changes between v_4 and v_2 silicate band, is also faster than control. It indicates a higher rate of pozzolanic reaction and produce higher amount of secondary CSH. The characteristic fly ash band also (1096 cm^{-1}) fades with time. As suggested by Berry et al.[24], pozzolanic reaction becomes dominant at ages after 28 days and result is a significant increase in compressive strength as compared to early ages and higher than control.

The higher rate of chloride diffusion allows reacting firstly with aluminium phases in fly ash forming Friedel's salt ($Ca_3Al_2O_6C_aCl_2.10H_2O$), which reduces the expansion. It improves the binding capacity of chlorides and reduce the amount of water soluble chloride[25]. The formation of Friedel's salt can be expressed through the following equation,

$$CaCl_2 + Ca_3Al_2O_6.6H_2O + 4 H_2O \rightarrow Ca_3Al_2O_6.CaCl_2.10H_2O \text{ (Friedel's salt)} \quad ...(11)$$

This result is well supported with the earlier report[3] who showed the blending 20% fly ash in OPC has higher strength than control and an increased resistance to sulphate attack.
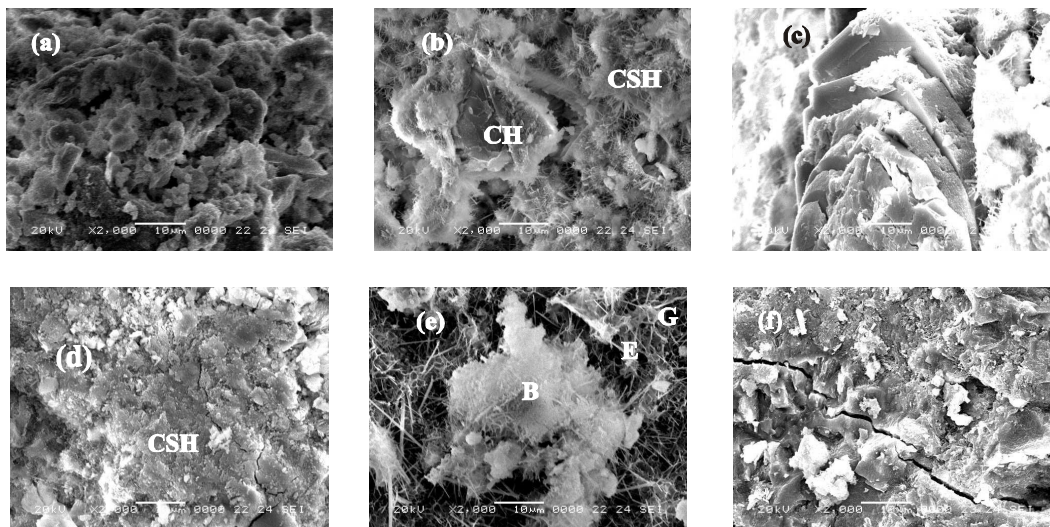

Fig. 4: SEM micrographs of control for (a) 1 hour, (b) 1 day, (c) 7 days (d) 28 days, (e) 90 days and (f) 180 days
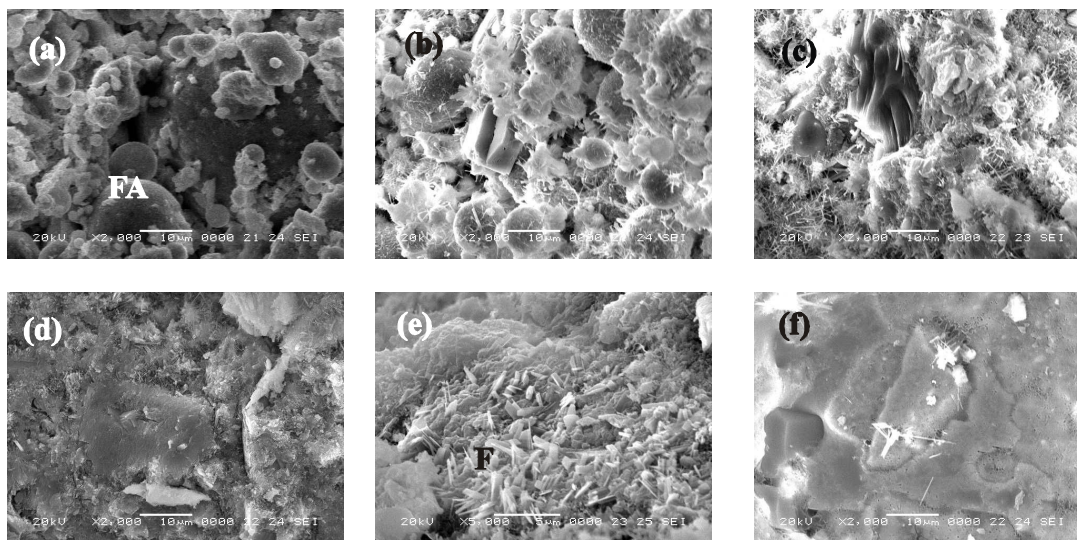
Fig. 5: SEM micrographs of blended composite for (a) 1 hour, (b) 1 day, (c) 7 days, (d) 28 days, (e) 90 days and (f) 180 days

SEM with EDS study

SEM micrographs of control and blended composite hydrated with sea water are shown in Figs. 4 and 5, respectively. From 1 hour micrograph (Fig. 4), polygonal shape of the cement particles[26] has produced textural changes on the surface, which is due to the starting of a hydration product like fine ettringite (E) needles[27]. In 1 day micrograph, the more randomly oriented ettringite needles, calcium silicate hydrate (CSH) and calcium hydroxide (CH) plates are clearly seen with large pores. At 28th day micrograph, the formation of CSH and CH occupies a large area with less pores compared to early stages. In matured ages (90th day), large amount of re-ettringite needles are clearly visible in a pore and continuously increases with time resulting in occurrence of cracking and disintegration of sample (180 days). Some recrystallized gypsum (G) and white deposit material (brucite, B)[28] are also seen in the micrographs. These products are confirmed by EDS spectra with a strong peak of Mg (Fig. 6a) indicating brucite[29]. The higher amount of Ca and S peaks (Fig. 6b) indicate the reformation of gypsum and higher Ca peak and smaller S and Al peaks (Fig. 6c), confirming the identification of re-ettringite[18].

In 1 hour blended composite (Fig. 5a), the fly ash particles consist of glassy spheres of various sizes[30]. In early stages, the rate of hydration is relatively low compared to control due to unreacted fly ash particles with more pores.

At 28th day, the fly ash particles react with CH plates indicating the start of pozzolanic reaction. This observation also agree well with the FTIR analysis. In 90th day micrograph, the fly ash and CH plates are low while the CSH content is higher. Also, more fine hexagonal slices were observed in pores due to formation of Friedel's salt (F)[31]. The EDS spectrum (Fig. 6d) also identifies the strong peaks of calcium, aluminium and chloride, which may be due to Friedel salt. This product prevents re-ettringite, recrystallisation of gypsum and brucite formation. The 180th day micrograph has more compacted structure of CSH due to more amount of secondary CSH formation (pozzolanic reaction).

The sulphate in seawater decreases the ingress of chloride into paste at early exposure. This is true for both; control and blended paste. It is observed that the gradual formation of ettringite needles in early exposure leads to compacted microstructure, which decreases the ingress of chloride to some extent. Also this experiment provides evidences that the presence of sulphate in seawater increases the ingress of chloride at later period. This was attributed to too much expansive ettringite needles and gypsum produced in pores. In blended composite, higher rate of chloride diffusion than sulphate ions, allows the chloride ions to react firstly with Al_2O_3 in fly ash to form Friedel's salt, which will reduce the formation of either recrystallisation gypsum or ettringite. The pozzolanic reaction due blended cement consume the $Ca(OH)_2$ content.
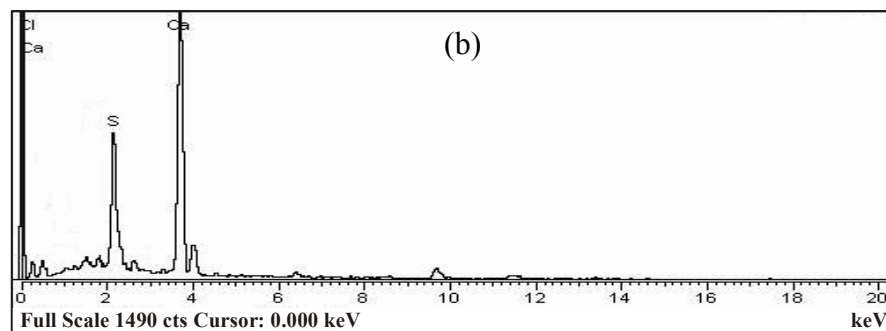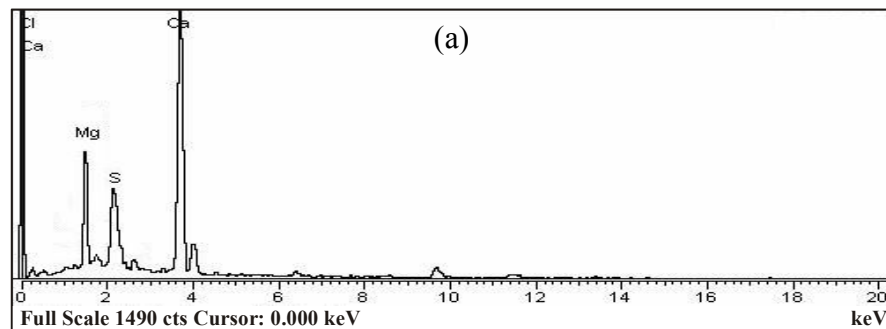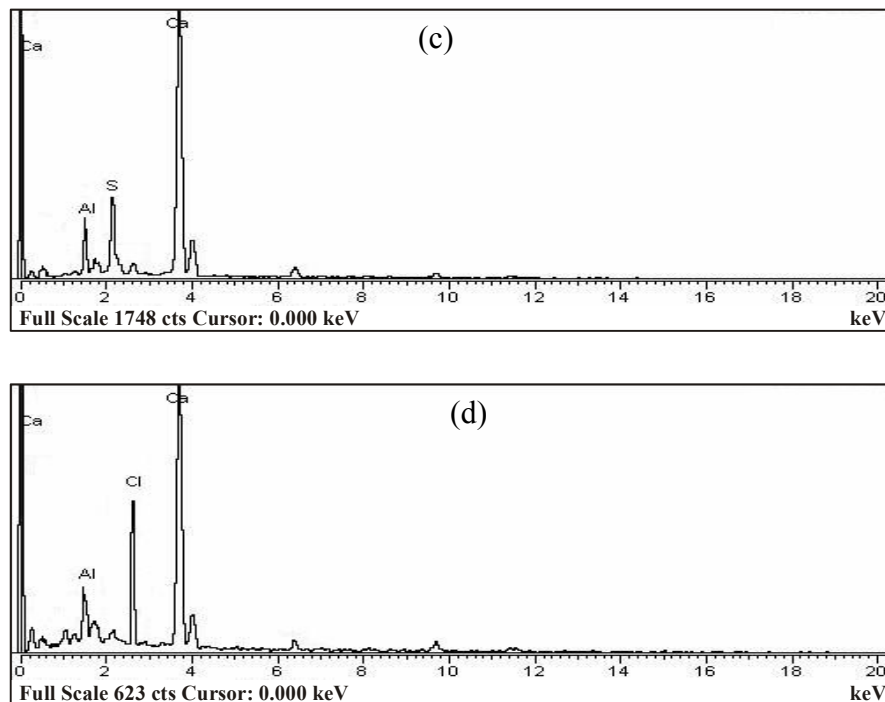
Fig. 6: EDS spectrum of (a) Brucite, (b) Gypsum (c) Ettringite needles and (d) Friedel's salt

CONCLUSION

The control has faster setting because of the formation of higher amount of ettringite formation than blended composite and at later period, strength is less due to sulphate attack. Blended composites reduce cementitious materials and hence, slow hydration and less strength at early stages are seen. After 28 days, pozzolanic activity of blended composites produce more amount of secondary CSH and hence, higher strength is there than control. Also, the presence of aluminate ions are (fly ash) more bound with chlorides to form insoluble Friedel's salt that reduces the alkalinity and does not accelerate the expansion. The 25% fly ash replacement cement has shown better corrosion resistance properties. This suggests the consideration of sea water as an alternative for potable water in the cementitious system.

ACKNOWLEDGEMENTS

Dept. of Structural Engg., Annamalai University for permitting them to measure the compressive strength.

REFERENCES

1.   C. A. Ferreira, Ribeiro and Ottosen, J. Hazar. Mater., **96**, 201 (2003).

2.   Snigdha Sushil and Vidya S. Batra, Fuel, **85**, 2676 (2006).

3.   Sunil Kumar, Cem. Concr. Res., **30**, 345 (2000).

4.   V. M. Malhotra and A. A. Ramezanianpour, CANMENT, 201 (1994).

5.   W. K. W. Lee and J. S. J. Van Deventer, Cem. Concr. Res., **32,** 577 (2002).

6.   Natalaya Shannhan and Abla Zayed, Cem. Concr. Res., **37,** 618 (2007).

7.   P. C. Mishra, V. K. Singh, K. K. Narang and N. K. Singh, Mater. Engg., **A357,** 13 (2003).

8.   M. A. Trezza and A. E. Lavat, Cem. Concr. Res., **31,** 869 (2001).

9.   U. S. Rai and R. K. Singh, Mater. Sci. Engg., **A392**, 42 (2005).

10.   M. Y. A. Mollah, Yu. Wenhong, R. Schennach and D. L. Coke, Cem. Concr. Res., **30,** 267 (2000).

11.   S. N. Ghosh and A. K. Chatterjee, J. Mater. Sci., **9,** 1577 (1974).

12.   Abdul Aziz A. Khalil, Cem. Concr. Res, **12,** 21 (1982).

13.   Tong Liang and Yang Nantu, Cem. Concr. Res., **24,** 150 (1994).

14.   F. Puertas and A. Fernández-Jiménez, Cem. Concr. Compo., **25,** 287 (2003).

15.   T. Van Gervan, Johnny Moors, Veroniek Dutre and Carlo Vandecasteele, Cem. Concr. Res., **34**, 1103 (2004).

16.   V. C. Farmer (Ed.), Mineral. Soc. Monogr, **4**. Mineralogical Society, London (1974).

17.   Manu Santhanam, Menashi Cohen and Jan Olek, Cem. Concr. Res., **36,** 132 (2006).

18.   M. Sahmaran, O. Kasap, K. Duru and I. O. Yaman, Cem. Concr. Compo., **29**, 159 (2007).

19.   Dražan Jozić and Jelica Zelić, Ceramic-Silikáty, **50,** 98 (2006).

20.   O. E. Gjørv and ø.Vennesland, Cem. Concr. Res, **9(2),** 229 (1979).

21. Tarek Uddin Mohemed, Hidenori Hamada and Toru Yamaji, Cem. Concr. Res., **34,** 593 (2004).

22. Shiqun Li, Jishan Hu, Lui Biao and Xinguo Li, Cem. Concr. Res., **34,** 753 (2004).

23. C. R. Shi and L. Day, Cem. Concr. Res., **28**, 197 (1995).

24. E. E. Berry, R. T. Hemmings and B. J. Cornelius, Cem. Concr. Compo, **12,** 253 (1990).

25. Jin Zuquan, Sun Wei, Zhang Yunsheng, Jiang Jinyang and Lai Jianzhong, Cem. Concr. Res., **37**, 1223 (2007).

26. Vagelis G. Papadakis, Cem. Concr. Res, **30,** 1647 (2000).

27. B. J. Dalgleish, P. L. Pratt and E. Toulson, J. Mater. Sci., **17**, 2199 (1982).

28. M. O. S. Farrell and B. B. Wild Sabir, Cem. Concr. Res., **30,** 757 (2000).

29. S. T. Lee, H. Y. Moon and R. N. Swamy, Cem. Concr. Compo., **27,** 65 (2005).

30. Byung-Wan Jo, Seung-Kook Park and Jong-Bin Park, Cem. Concr. Compo, **29,** 128 (2007).

31. Rui Luo, Yuebo Cai, Changyi Wang and Xiaoming Huang, Cem. Concr. Res., **33,** 1 (2003).